Molecular Crystals and Liquid Crystals
Publication details, including instructions for authors and subscription information:
http://www.tandfonline.com/loi/gmcl16

Two Kinds of Turbulent Flows in DSM of EHD Instabilities

Hideki Yamazaki [a] , Kazuyoshi Hirakawa [a] & Shoichi Kai [b]

[a] Department of Electronics, Kyushu University, Fukuoka, 812, Japan

[b] Department of Electrical Engineering, Kyushu Institute of Technology, Kitakyushu, 804, Japan

Version of record first published: 17 Oct 2011.

To cite this article: Hideki Yamazaki , Kazuyoshi Hirakawa & Shoichi Kai (1985): Two Kinds of Turbulent Flows in DSM of EHD Instabilities, Molecular Crystals and Liquid Crystals, 122:1, 41-57

To link to this article: http://dx.doi.org/10.1080/00268948508074741

Mol. Cryst. Liq. Cryst., 1985, Vol. 122, pp. 41–57
0026-8941/85/1224–41/$20.00/0

Two Kinds of Turbulent Flows in DSM of EHD Instabilities

HIDEKI YAMAZAKI and KAZUYOSHI HIRAKAWA

Department of Electronics, Kyushu University, Fukuoka 812, Japan

and

SHOICHI KAI

Department of Electrical Engineering, Kyushu Institute of Technology, Kitakyushu 804, Japan

(*Received August 3, 1984*)

We have observed two kinds of turbulent flows (DSM-like and DSM1), clearly showing transition phenomena between them, in the thin film of MBBA with a large aspect ratio (~170). To obtain quantitative properties of the spatial and temporal behavior of the phenomena, we have measured a spatial and temporal fluctuation of the flow pattern using image technique and analyzed it by Fourier transformation. We have observed the large difference of the structure of the spatial power spectrum between parallel ($P_{\parallel}$) and perpendicular ($P_{\perp}$) to the original WD roll direction. We have introduced the structural similarity factor $SI = 1/(1/n\sum_{i=0}^{n-1}|P_{\perp}(q_i) - P_{\parallel}(q_i)|^2)$ to describe the anisotropy of the spatial irregularity in the DSM flow, where q is the wave number. The factor SI drastically increases at the transition point, which means the decrease of a spatial anisotropy above that point. We have observed hysteresis in the factor with the applied voltage. The existence of the anisotropic turbulence with small SI may closely be related to the WD modes, i.e. initial director orientation.

Temporal Fourier analysis of the fluctuation has been done and a large increase in its power has been observed at the transition point. A power law decay, $1/f^2$ in the DSM-like and $1/f$ in the DSM1 regions, has been observed. It has been also observed in the transient region to the isotropic turbulence that the large scale intermittency occurs simultaneously in space and in time; showing coexistence of the temporal chaos and the spatial coherency. The results obtained show that the transition is a kind of the structural transition.

1. INTRODUCTION

Many studies on the onset of turbulence have theoretically[1–6] and experimentally[7–12] shown that there are several different routes of the

transition to chaos or turbulence. According to those, at least three quantitative different routes to chaos are found in moderate aspect ratio (Γ) systems; (i) period doubling bifurcation,[7–9] (ii) intermittency[10] and (iii) quasiperiodic convection with few incommensurate frequencies.[11] Such routes remarkably depend on Γ. In the case of the period doubling bifurcation, the experimental results are in good agreement with the theoretical expectations; for example the quantitative universality has been found by Feigenbaum.[4] Theoretical studies on intermittency have suggested the power law decay in the spectrum[5] and its dependence on burst near the onset point,[6] though, these suggestions have not been confirmed experimentally. In the case of (iii) both theoretical[2] and experimental[7,11] studies have not advanced so much as another cases.

So far, natures of the transition in moderate Γ system, typically less than 4, have described above. On the other hand, direct transition from steady state to chaos was reported in large Γ ($= 57$) system,[12] but it has not been clarified that the erratic phenomenon observed is transient one or not because of the very long characteristic time of the system. There is no work for a large Γ more than 100 as far as we know, except study for electrohydrodynamics (EHD) in a nematic liquid crystal. Therefore, the nature is not well known. Kai and coworkers[13–16] reported the successive transition from laminar to turbulent flow in the EHD instability; the Williams domain (WD), the grid pattern (GP), the quasi-GP and the dynamic scattering mode (DSM). They studied these transitions from a stand point of instability, analyzing the fluctuation of the transmitted light intensity (FTLI) passed through a cell. Their results concerning turbulent flow are following: (i) There are three types of chaos and/or turbulence; DSM-like, DSM1 and DSM2. (ii) The flow pattern is very complicated in the DSM-like region, though the macroscopic structure remains in a certain size. (iii) Anomaly of the fastest growing wave number q_{st}, large anomaly of the FTLI, softening of modes and critical slowing down occur at the DSM1 point. (iv) Long wavelength modes play an important role to the onset of turbulence. (v) Anomaly of the q_{st} occurs at the DSM-like and the DSM2 points; there is no quantitative difference observed between DSM-like and DSM1 except for q_{st}.

The studies mentioned above have dealt with temporal but spatial behaviors. Recently, we have reported the behaviors of the spatial modes in the transitions from WD to GP[17] and from GP to DSM-like[18] and that the transition in the latter case occurs via period doubling bifurcation in time and intermittency in space. We have

concluded that the DSM-like is a temporal chaos, because the chaos refers to the temporally erratic motion characterizing deterministic nonperiodic behavior.

One of the remaining problems interested is in the transition from DSM-like (temporal chaos) to DSM1 (turbulence). As far as we know, there are few experimental studies[15,16] on the temporal behavior in the transition between the two erratic states. The study on the spatial nature of flow pattern is necessary to understand the turbulent flow because it is erratic in time and in space. In this paper we describe the quantitative results obtained experimentally in the transition from DSM-like to DSM1. The study has been done through the observation and the analysis of both temporal and spatial behaviors in the flow patterns.

2. EXPERIMENTAL RESULTS AND DISCUSSIONS

2.1 Preparation

Experiment was worked out applying the advantageous properties of the nematic liquid crystal; (1) easy visualization of flow pattern due to the optical anisotropy, (2) easily controllable external stress (electric field), (3) shorter characteristic times (about 10^3 times shorter) than those in the case of the Rayleigh–Bénard convection.

The nematic liquid crystal used in the present study is MBBA (*p*-methoxybenzylidene-*p'*-*n*-butylaniline). It was enclosed in the thin cell consisting of two SnO_2 coated glass plates separated by polymer spacer. The dimensions of the cell were 15×10 mm^2 in area and 90 μm thick; the aspect ratio Γ is about 170. The measurements were made in the conduction regime at the temperature (25 ± 0.2)°C. The frequency of the applied voltage was 60 Hz. Hereafter the voltage V is normalized by V_c, $k = V/V_c$, the critical voltage at which the WD appears (in our case $V_c = 6.3$ volts). The block diagram of the experimental system is shown in Fig. 1. The optical signal passed through the cell is taken by the video camera and analyzed using the spatio-temporal image processing system made by the authors.[19] Figure 2 shows the photograph taken from the screen of the monitor TV. The bright line, whose location and length are able to be arbitrarily set, indicates a sequence of the sampling points (128 points in this case). Since the output signal of the video camera is proportional to the light intensity the temporal and the spatial information about flow patterns are obtained. The setting the sampling line and the data processing are done through the microcomputer.

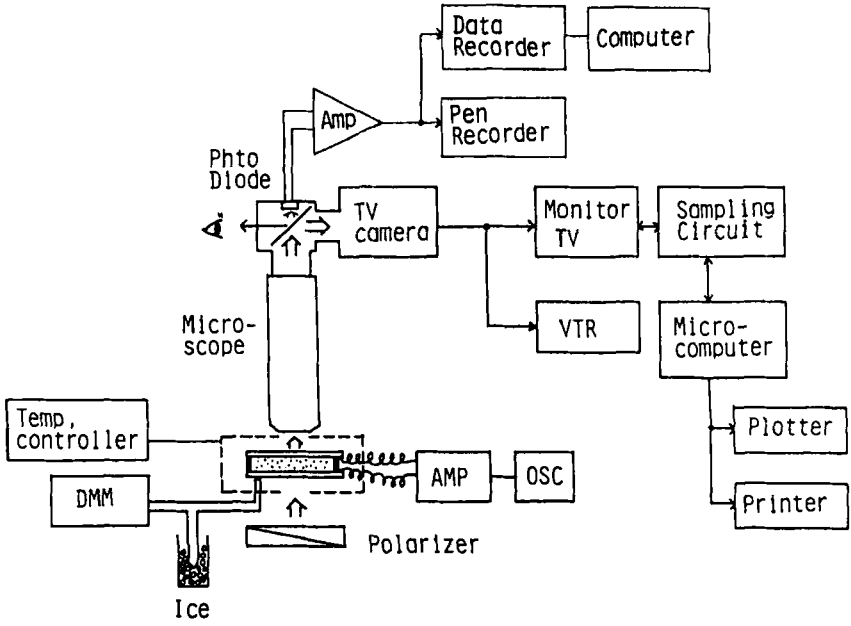

FIGURE 1 Experimental apparatus. The spatio-temporal image processing system is the part connected with the TV-camera in the right side.

In the present work, the spatial power spectra were obtained using this system. However, the study about the temporal behavior was done measuring the intensity of light covering a wide region (~3 mm^2) and in the duration about 3 minutes for each acquisition of datum.

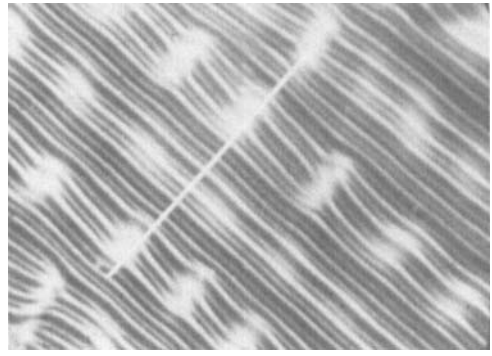

FIGURE 2 Photograph taken from the monitor TV screen. A bright straight line, whose length is 210 μm, indicates a sequence of sampling points (128 in this case).

2.2 Flow patterns

The nature of flow patterns in the successive transition under various conditions was studied in detail by the authors.[13, 17, 18] In Fig. 3 we explain the patterns related to our experiment; WD, DSM-like and DSM1. As shown in Fig. 3(a), the WD is straight striped pattern whose distance of every two lines is roughly equal to the depth of the cell.

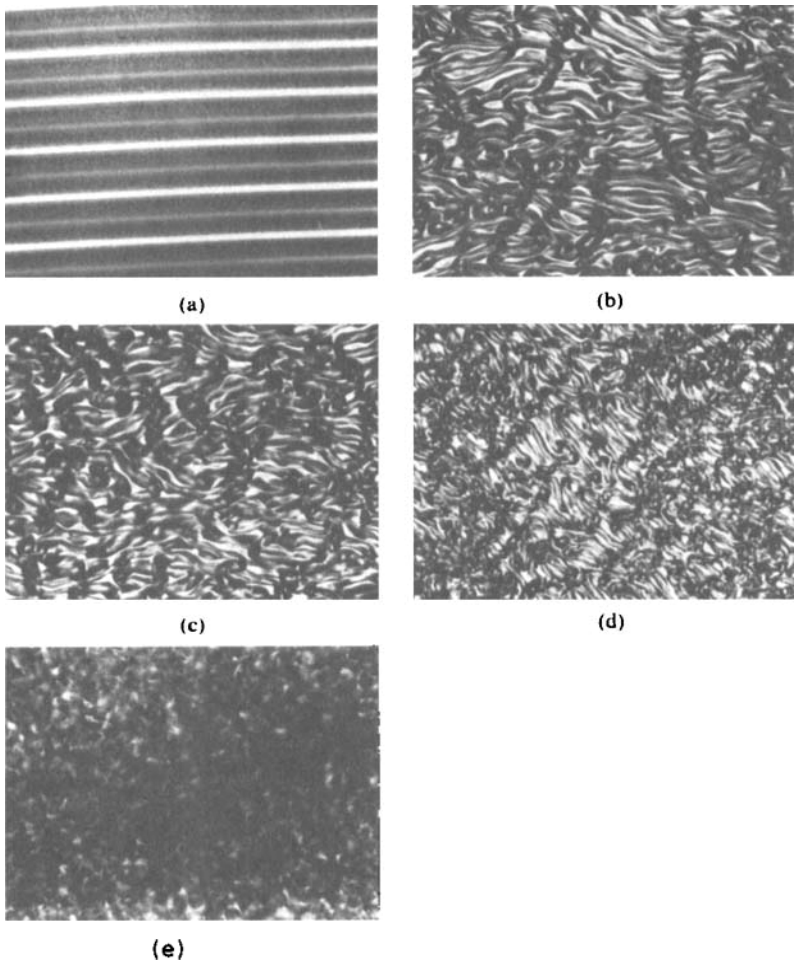

FIGURE 3 Flow patterns; (a) WD, (b) DSM-like (near the DSM-like point), (c) DSM-like (near the DSM1 point), (d) DSM1 (near the DSM1 point) and (e) DSM1 (fully developed turbulent state).

Slightly above the DSM-like point, although some large scale periodic structures remain along the direction parallel to the WD rolls, they are not stational, so that they vary complicatedly (see Fig. 3(b)). With increase in k, the size of those structures decreases and their shapes become complicated as shown in Fig. 3(c) (near the DSM1 point). Above but near the DSM1 point, there remain the structures observed in the DSM-like region. However, their shapes are more complicated and the area within which flow is complicated grows as seen in Fig. 3(d). Within this complicated region, disclination loops[21,22] being caught one another and moving irregularly are visible clearly under the crossed polarizers. No disclination loops can be visible in the DSM-like region.[22] With further increase in k, flow state turns to fully developed turbulence and only erratic motion and pattern are visible as seen in Fig. 3(e).

2.3. Spatial power spectrum

2.3.1. Spatial power spectrum at a fixed time. In the previous works we reported that one of the characteristics of the transitions from WD to GP[17] and from GP to DSM-like[18] is the difference in behaviors of the spatial modes obtained along the directions parallel and perpendicular to the WD rolls. In the present study, therefore, we measured the spatial power spectra for two directions ($P_\perp(q)$ and $P_\parallel(q)$) characterizing the flow patterns, where $\perp$ and $\parallel$ respectively indicate the directions perpendicular and parallel to the WD rolls. Here q is the wave number simply corresponding to the reciprocal of the length without 2π. The results are shown in Fig. 4.

As seen in Fig. 4(a) the shape of $P_\perp$ differs considerably from one of $P_\parallel$ near the DSM-like point; irregularity of the DSM-like is anisotropic in space. It is caused by the difference in the ordering structures along the two directions $\perp$ and $\parallel$ (see Fig. 3(b)). Wave numbers of the broad band modes q_B and q'_B are respectively inverses of the mean values of the lengths of the structures along the $\perp$- and $\parallel$-directions. The broadness in the spectrum indicates that there exists the non-stationary motion of the mode.

At $k \sim 4.7$, the mode q_B shifts to lower-q region and q'_B to higher one (see Fig. 4(b)). The shift of q_B comes from the increase of the intervals between structural domains; irregularly moving parts expand the intervals as seen in Fig. 3(c). The shift of q'_B comes from the decrement of the size of the structures. With further increase in k, the transition from DSM-like to DSM1 occurs. At $k \sim 5.6$ beyond the DSM1 point ($k = 5.14$), the mode q_B shifts further to lower q and the q'_B to higher q (Fig. 4(c)). As seen in Figs. 4(a), (b) and (c), the

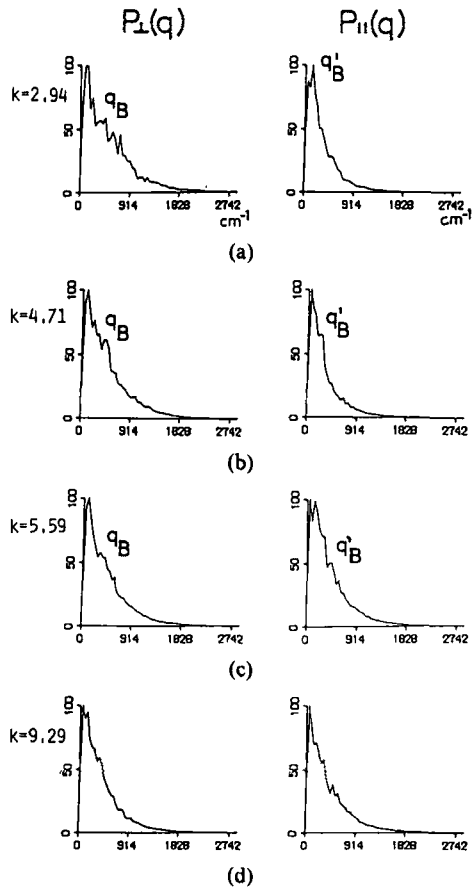

FIGURE 4 Spatial power spectra; (a) $k = 2.94$ (DSM-like), (b) $k = 4.71$ (DSM-like), (c) $k = 5.59$ (DSM1) and (d) $k = 9.29$ (DSM1). The data are averaged for 512 scenes under the same condition.

difference between the shapes of $P_\perp$ and $P_\parallel$ decrease with increase in k. This result shows that the difference of the spatial patterns observed along the two directions becomes smaller with the applied voltage, that is the flow changes from anisotropic to isotropic state. This behavior is observed visually under the microscope. The flow state with spatial coherency observed in the DSM-like region remains partially near the DSM1 point; small shoulders (q_B and q'_B) are seen in $P_\perp$ and $P_\parallel$ (see Fig. 4(c)). As k is far from the DSM1 point ($k > 6.5$), the flow becomes very complicated and isotropic turbulent state. At $k \sim 9.3$, the flow state is isotropic turbulence; the shape of $P_\parallel$ strongly resembles to that of $P_\perp$.

The results described above suggest that the difference between the shapes of $P_\perp$ and $P_\parallel$ decreases as irregularity of the flow pattern changes from anisotropic to isotropic. Hence, we introduce the similarity factor (SI) in order to show this aspect quantitatively;

$$SI = 1/\left(1/n \sum_{i=0}^{n-1} |P_\perp(q_i) - P_\parallel(q_i)|^2\right), \tag{1}$$

where $P(q_i)$ is the power of the ith wave number q_i and $n(= 64$ in our experiment) a half of the total number of the sampling points. This factor, therefore, gives the inverse of the mean distance between the two spectra $P_\perp$ and $P_\parallel$.

The plot of SI vs. k is shown in Fig. 5. The value of SI is small and nearly constant in the DSM-like region, but steeply increases near the transition point to the DSM1. Although scatters of SI are pretty large, it is clear that the mean value of SI is large and tends to saturate at a large k. Hysteresis is also seen in both SI and TLI (see Fig. 7) near the transition point from DSM-like to DSM1. This result suggests that the transition from DSM-like to DSM1 is inverted-bifurcation with higher-order terms (i.e. so called the first-order-like phase transition). As far as we know any hysteresis has not been found in the successive transition in hydrodynamic instabilities. We conclude that the DSM1

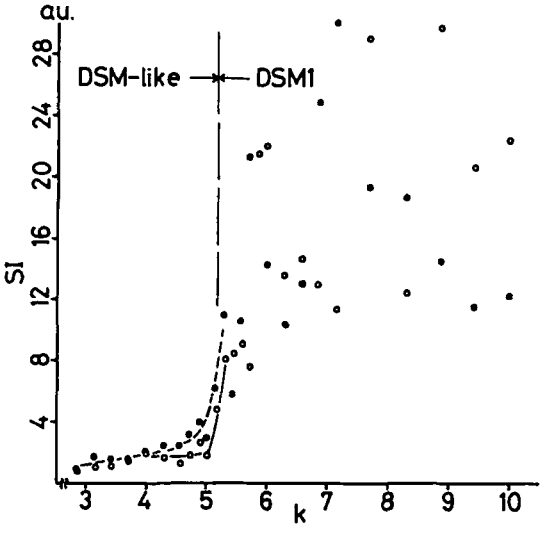

FIGURE 5 The k-dependence of the similarity (SI). ○; increasing k and ●; decreasing k. Hysteresis is clearly seen near the transition point. The applied voltage is increased 0.5 volts every 30 minutes.

is the isotropic turbulent flow and the transition form DSM-like to DSM1 is a first-order-like transition.

2.3.2. The temporal change of the spatial spectrum. Flow pattern changes from time to time. Especially it is strong in the fully developed turbulent region. Thus the scatters of *SI* are large in higher k region. To know this aspect quantitatively, we measure the temporal change of the spectra for both $P_\perp$ and $P_\parallel$. We call this quantity the fluctuation factor of the spectrum (FFS);

$$FFS = 1/m \sum_{j=1}^{m} 1/n \sum_{i=0}^{n-1} |P^{AVE}(q_i) - P^j(q_i)|^2,$$
$$P^{AVE}(q_i) = 1/m \sum_{j=1}^{m} P^j(q_i), \qquad m = 512, \quad n = 64, \tag{2}$$

where $P^j(q_i)$ denotes the jth power measured at a fixed k. This factor, therefore, gives the variance in the shapes of the spectra changing temporally.

Figure 6 shows the k-dependence of the *FFS*, the value of which in $P_\parallel$ is larger than that in $P_\perp$ within the DSM-like region. This fact indicates that temporal change of modes along the direction parallel

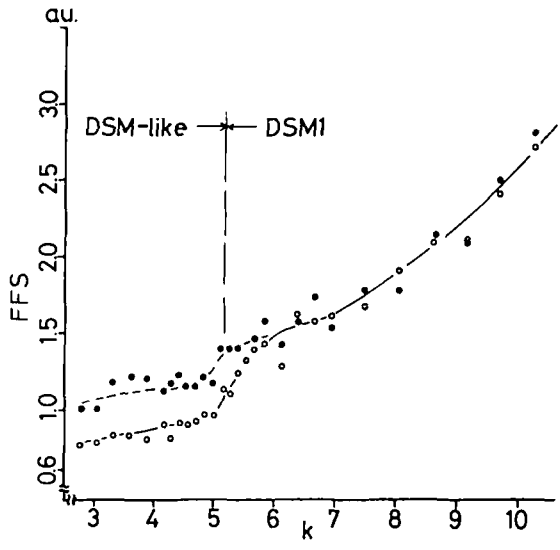

FIGURE 6 The k-dependence of the fluctuation factor of the spectra (FFS) along the directions perpendicular and parallel to the WD rolls. ○; perpendicular direction and ●; parallel direction.

to the WD rolls is larger than that perpendicular to the WD rolls; the fluctuation in the ordered structure seems to be large in the parallel direction than in the perpendicular one. The difference of the *FFS* between two directions becomes small as the irregularity of the flow changes from anisotropic to isotropic one (see Fig. 6). The *FFS* becomes large with the transition from DSM-like to DSM1 and increases monotonously as the state goes from the DSM1 point into fully developed DSM. The large value of *FFS* causes the large scatters of *SI* in the higher k region. The intensity of the *FFS* is proportional to the fluctuation of the temporal change of the spatial structures. Thus this result shows that both spatial and temporal fluctuation are nonperiodic and irregular in the high k region.

2.4. Temporal behaviors

We analyzed the fluctuation of the transmitted light intensity (TLI) to study the relation between spatio-temporal behavior and the origin of anomalous FTLI with the transition from DSM-like (temporal chaos) to DSM1 (turbulent flow).

2.4.1. Fluctuation of the transmitted light. Figure 7 shows the k-dependence of the TLI and the second moment of the FTLI,

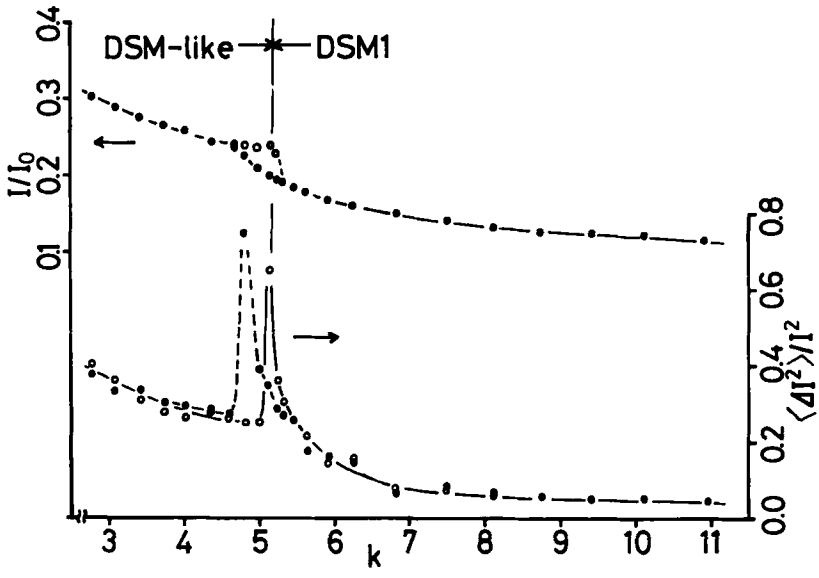

FIGURE 7 The k-dependence of the transmitted light intensity (I/I_0) and the second moment of the fluctuation ($\langle \Delta I^2 \rangle / I^2$). ○; increasing k and ●; decreasing k. I_0 is the transmittancy at $k = 0$.

$\langle \Delta I^2 \rangle / I^2$, where I is the TLI and $\langle \Delta I^2 \rangle$ the variance of the FLTI. The TLI decreases suddenly at the DSM1 point. Moreover, there is a clear hysteresis near the transition point. A large anomaly as well as one observed in the previous experiment[14, 15] is clearly seen in the neighborhood of the transition point ($k_1 = 5.14$). In our case, however, the anomaly occurs suddenly at k_1; the fluctuation is large in the region from the transition point to slightly higher k. The hysteresis is clearly seen also in the FTLI like one in the TLI and *SI*. Therefore, we conclude that the transition from DSM-like to DSM1 is inverted-bifurcation (the first-order-like transition), though the origin of the hysteresis is not clarified at the present. The origin of the anomalous FTLI will be described later.

2.4.2. Temporal power spectrum. The anomaly of the FTLI at k_1 suggests the appearance of the mode with very low frequency. Figure 8 shows the typical examples of the temporal power spectra in the region from DSM-like to DSM1. At $k \sim 3.8$ (near the middle point between the DSM-like and DSM1), there are few broad band modes in a low frequency region; i.e. the flow is complicated (see Fig. 8(a)). The inset given in upper right part of Fig. 8(a) shows that the spectrum is divided into three frequency ranges; (I) low (< 0.3 Hz), (II) intermediate ($0.3 - 3$ Hz) and (III) high ranges (> 3 Hz). At $k \sim 5.1$ (just below the DSM1 point), the shape of the spectrum is still nearly equal to one obtained at $k \sim 3.8$ as seen in Fig. 8(b). Figures 8(a) and (b) show that spectra in the DSM-like region have following features; (1) constant power in the range (I), (2) $1/f^2$-type spectrum in (II) and (3) $1/f^n$-type ($n > 3$) spectrum in (III) where n decreases gradually with increase in k. This result suggests that the range (III) differs from (I) and (II). As the transition to DSM1 occurs, the shape of the spectrum changes drastically (see Fig. 8(c)). It should be noted that at $k = 5.14$ (the DSM1 point), a very low frequency mode f_0 appears and the spectrum simultaneously changes from $1/f^2$-type to $1/f$-one over the ranges (I) and (II). The appearance of the mode f_0 which was also observed in the previous experiment[14, 15] meets the expectation from the result in the FTLI. In our experiment, however, the mode f_0 is always seen in the whole ranges of the DMS1 (see Fig. 8(d)). Therefore, we think that the mode f_0 is indispensable to maintain the turbulent flow. The temporal scale of the mode f_0 seems to be related to the characteristic time due to the fluctuation of charge in horizontal direction as discussed in the previous paper.[18] The superior direction of this mode appears to be parallel to the WD rolls. Contrary to this, the direction of the lateral mode in the DSM-like seems to be mainly perpendicular to the WD rolls.

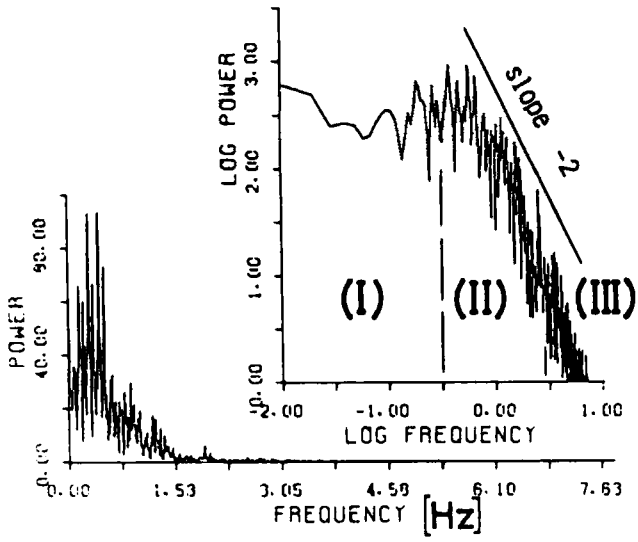

(a)

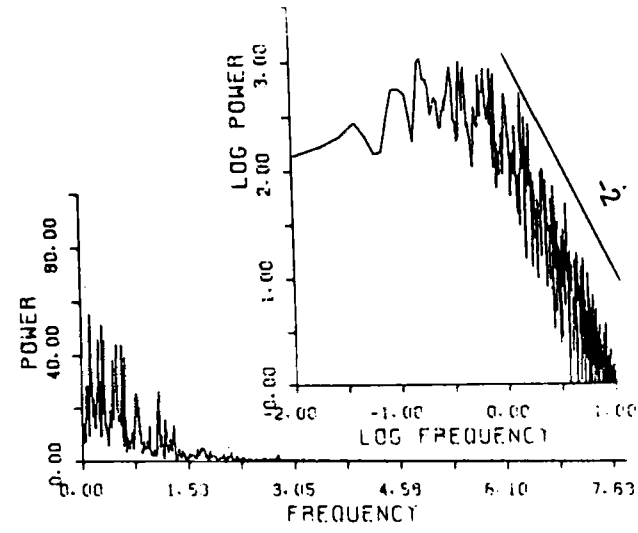

(b)

FIGURE 8 Temporal power spectra; (a) $k = 3.81$ (DSM-like), (b) $k = 5.08$ (DSM-like), (c) $k = 5.24$ (DSM1) and (d) $k = 10.3$ (DSM1). The insets in the upper right sides show the log-log plot of the spectra.

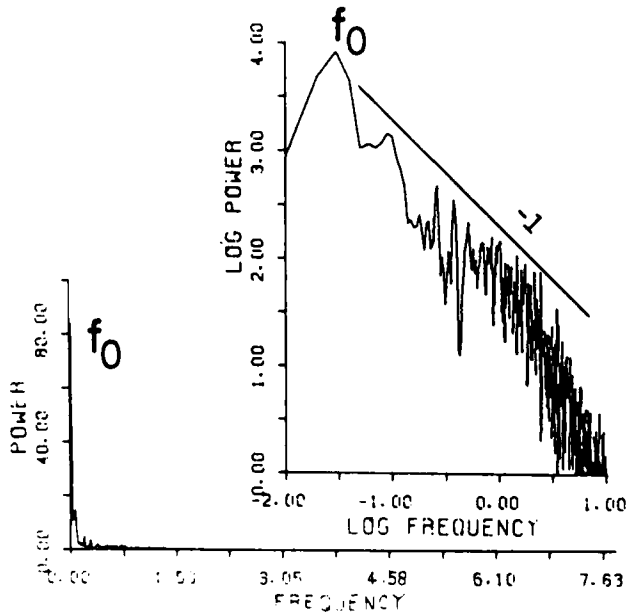

(c)

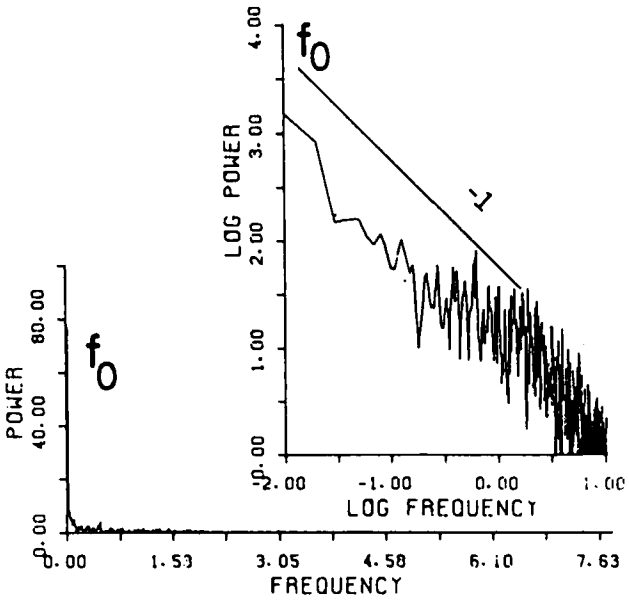

(d)

Manneville[5] showed numerically that as the chaos occurs via intermittency the $1/f$-type spectrum over wide frequency range is obtained near the transition point. The $1/f$-type spectrum obtained in our experiment is kept from the onset point to fully developed turbulent state. It differs from the theoretical prediction by Manneville. Shobu, Ose and Mori[6] showed that the power spectrum of intermittency near its onset point obeys the power law $1/f^2$ or $1/f^4$ in a small frequency region and has a tail of the form $1/f^2$ in the case of phase bursts. On the other hand, Ahlers and Behringer[12] observed the power law decay in the spectra in the turbulent state, but the details have not been clarified; their power law differs from ours. Malraison and Atten[20] has obtained another power law measuring the dc-current fluctuation in EHD. They observed the intermittent behavior in viscous dominant region. However, their results also differ from ours. No spatial information about the fluctuation have been obtained. Even though, the observation of such intermittent fluctuations suggests high possibility of the existence of the spatially coherent intermittency. Such an intermittency would correspond to our f_0 mode.

2.4.3. Intermittency. Figure 9 shows the examples of the temporal evolution of the FTLI beyond the DSM1 point. As seen in the figure the amplitude and the mean interval between anomalous

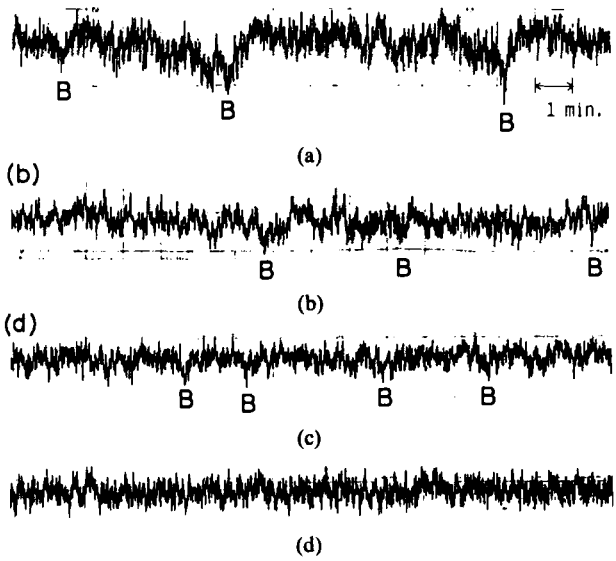

FIGURE 9 The time evolutions of the FTLI's beyond the DSM1 point; (a) $k = 5.14$ (the DSM1 point), (b) $k = 5.51$, (c) $k = 5.88$ and (d) $k = 6.65$.

fluctuation (denoted by B) are the largest at the DSM1 point. The interval (the modes f_0) shortens with increase in k keeping randomness.

In order to know the relation between the fluctuation and the flow pattern, we have taken photographs of the pattern simultaneously with the measurement of the FTLI. We can see in Fig. 10 that the large decrease of the FTLI (denoted by B) is caused by the appearance of the complicated pattern over a wide area. The flow in these

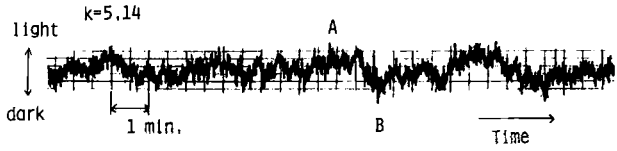

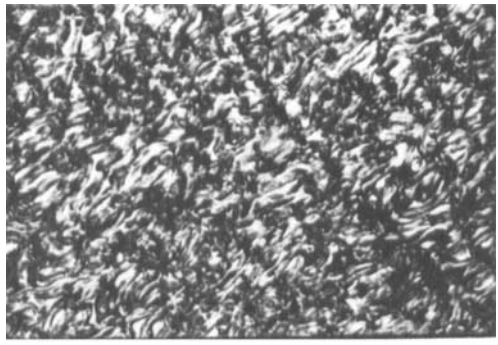

(a)

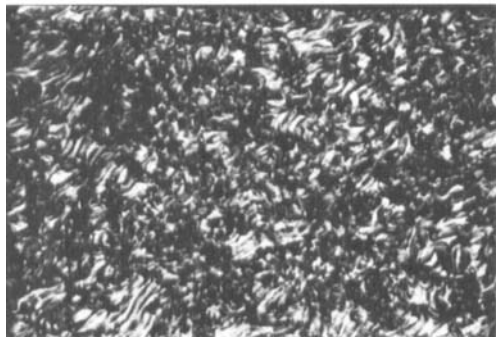

(b)

FIGURE 10 The FTLI and the patterns. The photographs (A) and (B) were taken respectively at A and B shown in the temporal change of the FTLI (A; light, B; dark).

complicated areas is erratic and makes many disclination lines with closed loop. On the other hand, the remaining ordered structure is seen near the center in the photograph (A). Since these complicated areas grow up with increase in the applied voltage, the mean interval of the large fluctuation (denoted by B also in Fig. 9), the TLI and the scale of the fluctuation are reduced. The intermittent behavior is not clearly seen in Fig. 10, because the DSM1 consists of many scales of flow. However, the k-dependence of the FTLI (Fig. 9) and flow patterns (Fig. 10) suggest the existence of the spatial intermittency near and beyond the DSM1 point.

3. CONCLUSION

We have observed two kinds of turbulent flows (DSM-like and DSM1), clearly showing transition phenomena between them, in the film of MBBA with a large aspect ratio ($\sim$170). The quantitative properties have been obtained by Fourier analysis of a spatial and temporal fluctuation of the flow pattern. The concluding remarks obtained in the present study are as follows:

1. The differences between the DSM-like and the DSM1 are seen in (i) the shapes of the spatial power spectra in the direction perpendicular and parallel to the WD rolls and (2) power law decay in the temporal power spectra.
2. The irregularity in the DSM-like is anisotropic in space.
3. The anisotropic irregular flow turns to the isotropic one to compensate the modes which do not exist in each direction in the former phase.
4. Hysteresis is observed as the transition from DSM-like to DSM1 occurs.
5. The transition to fully developed turbulence occurs by breakdown of spatial coherency.
6. The fluctuation of the transmitted light intensity shows anomaly at the transition point.
7. The power law decay of the temporal spectrum changes from $1/f^2$ to $1/f$ with the transition from DSM-like to DSM1.
8. Temporal chaos and spatial coherency coexist in the transient region to the isotropic turbulence. Such a coexistence creates sometimes intermittent behavior.
9. The very low frequency mode f_0 is strongly related to the generation of the turbulent flow.

The authors express their hearty thanks to Mr. T. Murata and Mr. K. Yoneda for their assistance in the experiment.

References

1. L. D. Landau and E. M. Lifshitz, *Fluid Mechanics* (Pergamon, London, 1959).
2. D. Ruelle and F. Takens, *Commun. Math. Phys.* **20**, 167 (1971).
3. R. M. May, *Science* **186**, 645 (1974).
4. M. J. Feigenbaum, *J. Stat. Phys.* **19**, 25 (1978).
5. P. Manneville, *J. de Phys.* **41**, 1235 (1980).
6. K. Shobe, T. Ose and H. Mori, *Progr. Theor. Phys.* **71**, 458 (1984).
7. J. P. Gollub and S. V. Benson, *J. Fluid Mech.* **100**, 449 (1980).
8. M. Giglio, S. Musazzi and U. Perini, *Phys. Rev. Lett.* **4**, 243 (1981).
9. A. Libchaber, C. Laroche and S. Fauve, *J. de Phys. Lett.* **43**, 211 (1982).
10. A. Libchaber and J. Maurer, *Nonlinear Phenomena at Phase Transitions and Instabilities* ed T. Riste, (Plenum Press, 1981).
11. M. Sano and Y. Sawada, private communication.
12. G. Ahlers and R. W. Walden, *Phys. Rev. Lett.* **44**, 445 (1980).
13. S. Kai and K. Hirakawa, *Mem. Fac. Engin. Kyushu Univ.* **36**, 269 (1977).
14. S. Kai and K. Hirakawa, *Progr. Theor. Phys. Suppl.* **64**, 212 (1974).
15. S. Kai, M. Araoka, H. Yamazaki and K. Hirakawa, *J. Phys. Soc. Jpn.* **46**, 393 (1979).
16. S. Kai, M. Araoka, H. Yamazaki and K. Hirakawa, *J. Phys. Soc. Jpn.* **46**, 401 (1979).
17. H. Yamazaki, S. Kai and K. Hirakawa, *J. Phys. Soc. Jpn.* **52**, 1878 (1983).
18. H. Yamazaki, S. Kai and K. Hirakawa, *Mem. Fac. Engin. Kyushu Univ.* (in print).
19. M. Sato, M. Takada, H. Yamazaki, S. Kai and K. Hirakawa, *Tech. Rep. Kyushu Univ.* **55**, 641 (1982) (in Japanese).
20. B. Malraison and P. Atten, *Phys. Rev. Lett.* **49**, 723 (1982).
21. J. Nehring and M. S. Petty, *Phys. Lett.* **40A**, 407 (1972).
22. T. Krupkowski and W. Ruszkiewicz, *Mol. Cryst. Liq. Cryst.* **49**, 47 (1978).